



## Discover Generics

Cost-Effective CT & MRI Contrast Agents



WATCH VIDEO

# AJNR

### **Transorbital color Doppler flow imaging of the carotid siphon and major arteries at the base of the brain.**

H H Hu, C L Luo, W Y Sheng, M M Teng, W J Wong and Y O Luk

This information is current as of June 4, 2025.

*AJNR Am J Neuroradiol* 1995, 16 (3) 591-598  
<http://www.ajnr.org/content/16/3/591>

# Transorbital Color Doppler Flow Imaging of the Carotid Siphon and Major Arteries at the Base of the Brain

Han-Hwa Hu, Chau-Lin Luo, Wen-Yung Sheng, Michael Mu-Huo Teng, Wen-Jang Wong, and Yun-On Luk

**PURPOSE:** To describe and evaluate an application of sonography, transorbital color Doppler flow imaging of the carotid siphon and major intracranial arteries, and to compare it with transtemporal color Doppler flow imaging. **METHODS:** The carotid siphon and major arteries at the base of the brain of 50 healthy volunteers were screened using the transorbital color Doppler flow sonography. These arteries were also studied by a transtemporal approach for comparison. In 5 volunteers, MR images in special inclination planes were obtained and compared with the transorbital color-coded Doppler flow images. **RESULTS:** The B-mode image of the orbit and intracranial anatomic structures, in addition to the color-coded flow images, provided an unambiguous identification of the carotid siphon and major intracranial arteries. The failure rate was lower when using the transorbital approach than when using the transtemporal approach in identifying the anterior cerebral artery (17% versus 32%). Color Doppler flow imaging using the transtemporal approach was better for the middle cerebral artery, whereas color Doppler flow imaging using the transorbital approach was better for the anterior cerebral artery (contralateral). The Doppler incident angles using the transorbital approach were better for the carotid siphon and anterior cerebral artery (contralateral). **CONCLUSION:** Transorbital color Doppler flow imaging, when used in conjunction with the transtemporal examination, can add information concerning the major arteries at the base of the brain.

**Index terms:** Ultrasound, Doppler; Ultrasound, technique; Arteries, cerebral; Arteries, ultrasound

*AJNR Am J Neuroradiol* 16:591–598, March 1995

Color Doppler flow sonography has been documented as a noninvasive method for the examination of the intracranial arteries (1–6). It is possible to obtain flow information and images of the basal cerebral arteries by the transtemporal approach (1–4). However, Doppler examination with this approach fails in patients with poor acoustic windows (7–10). The transorbital approach may be an alternative or complementary diagnostic method for these patients. This article describes the instruments

and techniques of transorbital color Doppler flow sonography. Results using the transorbital and transtemporal approach are compared.

## Subjects and Methods

Fifty volunteers (32 men and 18 women, 38 to 79 [mean,  $56 \pm 12$ ] years of age) were examined with color Doppler flow imaging using the transorbital method for detecting the carotid siphon and major arteries at the base of the brain. There was no history or physical signs of cerebrovascular disease, and extracranial arterial disease was excluded by color Doppler flow sonography. The carotid siphon and major arteries at the base of the brain were also examined by the transtemporal approach for comparison. A computed sonography system (Acuson 128 XP, Mountain View, Calif) with a dual-frequency 2.0/2.5 MHz sector scan transducer with a 19-mm aperture was used. Magnetic resonance (MR) angiography was done on 5 volunteers for identification and comparison of the courses of the various segments of the carotid siphon and major arteries at the base of the brain. MR angiography was performed on a 1.5-T system, using three-dimensional time of flight and the following parameters: 40/

---

Received March 8, 1994; accepted after revision August 13.

Supported in part by grants from the Yen Tjing Ling Medical Foundation of the Veterans General Hospital-Taipei and the National Science Council of the Republic of China.

From the Neurological Institute (H.-H.H., C.-L.L., W.-Y.S., W.-J.W., Y.-O.L.) and the Department of Radiology (M.M.-H.T.), Veterans General Hospital-Taipei, Yang-Ming Medical College, Taiwan, Republic of China.

Address reprint requests to Han-Hwa Hu, MD, Neurological Institute, Veterans General Hospital-Taipei, Taiwan, 11217, Republic of China.

*AJNR* 16:591–598, Mar 1995 0195-6108/95/1603-0591

© American Society of Neuroradiology

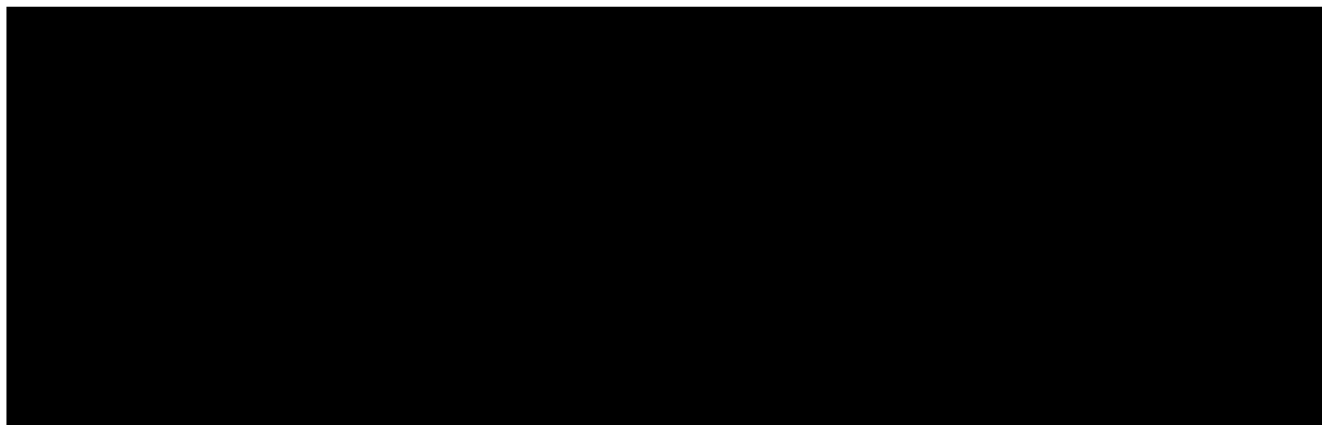


Fig 1. A, Two principal directions for transducer application over the eyelid. The letter (a) indicates the axial scan with the ultrasound beam directed in an anteroposterior direction ( $5^{\circ}$  to  $10^{\circ}$  with the sagittal plane); (b) indicates the axial scan with transducer tilted obliquely and the ultrasound beam directed to the roof of the orbit.

B, In anteroposterior direction, the lateral and the medial walls of the orbit appear symmetrical in B-scan. Color flow signals from the ophthalmic artery (*red*), supraclinoid portion (*blue*), and genu and cavernous sinus portion (*red*) of the carotid siphon may be obtained.

C, In oblique direction, the orbital walls in the B-scan appear asymmetrical and the medial wall is longer than the lateral. The color flow signals from both anterior cerebral arteries and both middle cerebral arteries could be obtained. The letter a indicates cavernous sinus portion of carotid siphon; b, supraclinoid portion of carotid siphon; c, ophthalmic artery; d, ipsilateral anterior cerebral artery; e, contralateral anterior cerebral artery; f, ipsilateral middle cerebral artery; g, contralateral middle cerebral artery; h, anterior communicating artery; i, ipsilateral posterior communicating artery; j, contralateral posterior communicating artery; k, ipsilateral posterior cerebral artery; l, contralateral posterior cerebral artery; and G, globe.

4.4/2 (repetition time/echo time/excitations);  $25^{\circ}$  flip angle; field of view, 16 to 24 cm;  $256 \times 192$  matrix; and 1-mm section thickness. MR angiography could be reconstructed according to the geographic plane of sonographic image.

To test the reproducibility of the transorbital color Doppler flow imaging, 10 volunteers whose carotid siphon and all major arteries at the base of the brain were successfully detected by the first examiner underwent transorbital color Doppler flow imaging 1 week later by a second examiner who had no knowledge of the results of the first examination. Agreement between the two examiners was tested by intraclass correlation.

The subjects were examined in the supine position. They were instructed to turn their eyes away from the transducer to avoid the refractive power of the ocular lenses. After covering the closed eyelids with gel, the transducer was applied without pressure on the superior or lateral orbital rim. The ultrasound beam was directed at the apex of the orbit in either an anteroposterior direction through the superior orbital fissure and the optic canal or in an oblique direction through the roof of the orbit. The low-transmission-output power setting ( $<25$  or  $<50$  mW/cm $^2$ ) was used, and the gain level was augmented in B mode and color-coded Doppler to obtain a clear picture of the orbital and basal cerebral structures and color Doppler image of the targeted cerebral arteries. Color assignment depends on direction of flow and is selectable by the operator. Flow toward the transducer was assigned as red and flow away from the transducer as blue. The maximum estimated in situ spatial peak temporal average intensity with a power setting at less than 25 mW/cm $^2$  was 9.7

mW/cm $^2$  in the color imaging mode and 9.1 mW/cm $^2$  in pulsed Doppler examination; at less than 50 mW/cm $^2$ , this maximum was 29 mW/cm $^2$  for both the color imaging mode and pulsed Doppler. The maximum estimated in situ spatial peak temporal average intensity at  $-6$  dB was 14.5 mW/cm $^2$  for B-mode imaging. To avoid prolonged insonation to the eye, the maximal insonation time was 20 minutes for one eye. Arteries not identified in this time interval were considered as failures.

By using the anteroposterior transorbital approach (Fig 1A and B), the cavernous sinus portion (C-3) and supraclinoid portion (C-1) of the internal carotid artery (ICA) were clearly demonstrated. The oblique transorbital direction (Fig 1A and C) provided clear images of the ipsilateral middle cerebral artery (MCA), anterior cerebral artery (ACA), the contralateral ACA and MCA, anterior communicating artery, and contralateral posterior communicating artery when active. Furthermore, the flow signals of both posterior cerebral arteries could also be obtained in some subjects.

Peak systolic and end-diastolic flow velocities were measured, and the pulsatility indices were calculated in various segments of the carotid siphon, ACA, and MCA. The pulsatility indices were represented by a resistance index and A/B ratio (11). The angle between the vascular axis and the ultrasonic beam was measured to calculate an angle-corrected blood-flow velocity. This procedure required careful observation of the course of the artery. In individual cases, an unfavorable incident angle of greater than  $64^{\circ}$  could be observed, and an incident angle of less than  $65^{\circ}$  is possible by rotating and tilting the transducer. Unfavorable angles of greater than  $64^{\circ}$  were excluded from

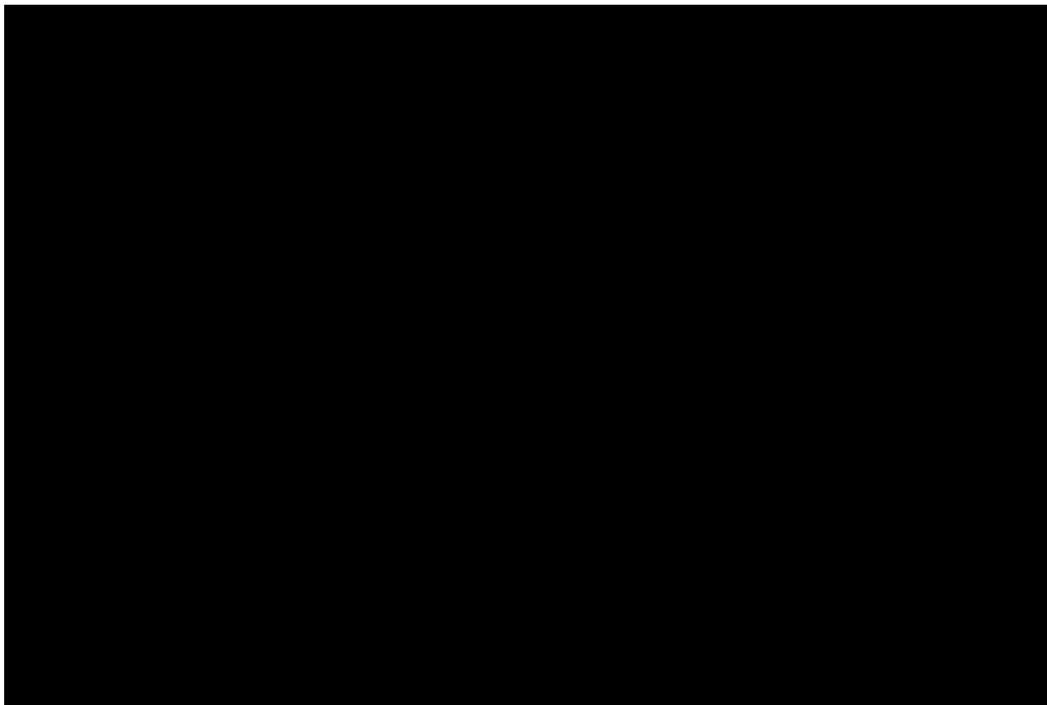


Fig 2. A, Doppler flow imaging of the carotid siphon and ophthalmic artery obtained from anteroposterior direction of transorbital examination.

B, MR angiography of the same subject in corresponding tomographic plane. The letter *a* indicates cavernous sinus portion of carotid siphon; *b*, supraclinoid portion of carotid siphon; *c*, ophthalmic artery; and *G*, globe.

the calculations of the blood-flow velocities. Pulsed Doppler measurements were taken at the approximate anatomic site if the color flow imaging of some portions of the carotid siphon and major arteries at the base of the brain did not appear in the B-mode scan. The pulsatility indices and the spectrum of Doppler shifts were used as references for those cases of either an unknown or unfavorable incident angle.

Results were expressed as the mean value and the standard deviation. The Student's *t* test was used for the comparison of the flow velocities and incident angles between the transtemporal and transorbital approach. McNemar's  $\chi^2$  test was used for the comparison of the failure rates between the two approaches. For all tests,  $P < .05$  was considered statistically significant.

## Results

Comparisons of the ultrasound images and the MR angiography images revealed evident agreement for artery identification (Figs 2A and B, 3A and B, and 4A and B).

The ultrasound images of the transorbital approach from the anteroposterior direction, and the lateral and medial walls of the orbit, appeared symmetrical in the B-mode scan. Color Doppler flow signals from the ophthalmic artery (OA) were imaged as a longitudinal color-

coded red line at the apex of the orbit. Tracing the OA signal deeper, the genu of the carotid siphon and the junction of the OA and ICA could be found by tilting the transducer upward slightly (Figs 1B and 2A and B). The color flow signals of the supraclinoid portion of the ICA (C-1) were blue if there was not aliasing. Moreover, the cavernous sinus portion of the ICA (C-3) could be seen by tilting the transducer slightly downward. This segment appeared as a red color. The origin of the OA and the various portions of the carotid siphon could be identified by tilting and rotating the transducer.

From the oblique direction of the transorbital approach, the orbital walls in the B-scan appeared asymmetrical and the medial wall was observed to be longer than the lateral wall (Fig 1C). Color flow signals from the precommunicating segment (A-1) of the contralateral ACA were very easily delineated as a longitudinal color-coded red line inferior and medial to the medial wall. The ipsilateral A-1 of the ACA and both postcommunicating segments (A-2) of the ACA and the MCA could then be identified by slightly rotating and tilting the transducer (Figs 1C, 3A and B, and 4A and B). The color flow

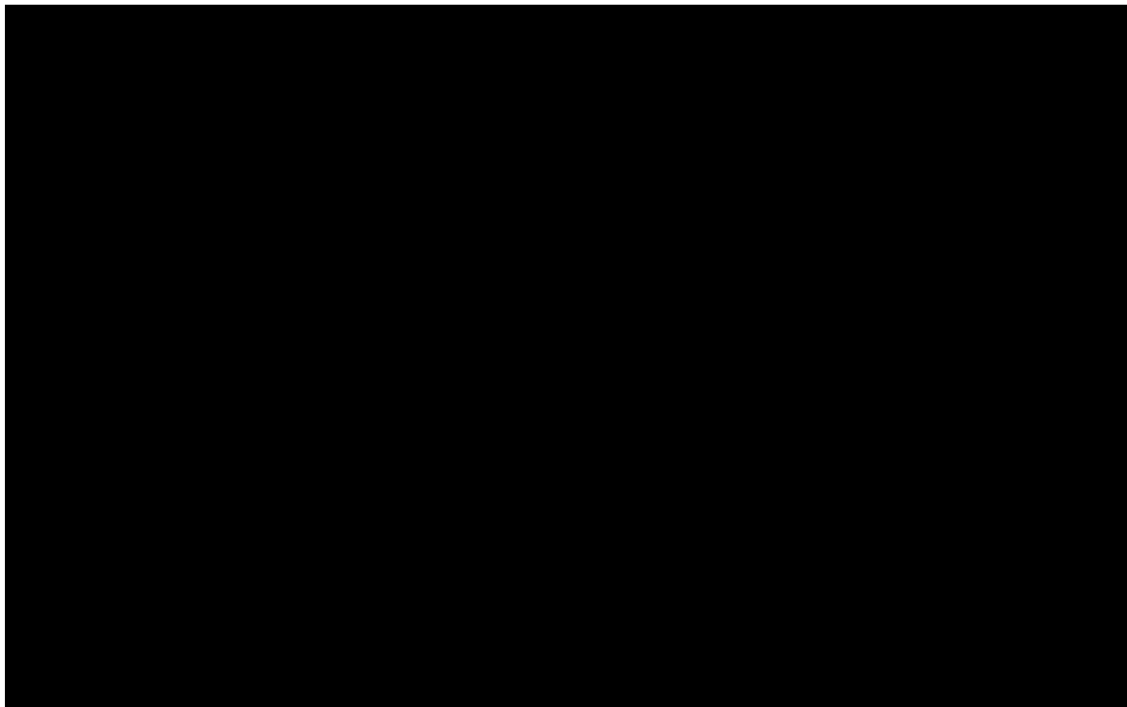


Fig 3. A, Doppler flow imaging of both anterior cerebral arteries and both middle cerebral arteries from an oblique transorbital examination.

B, MR angiography of same subject in corresponding tomographic plane. The letter *a* indicates ipsilateral anterior cerebral artery; *b*, contralateral anterior cerebral artery; *c*, contralateral middle cerebral artery; *d*, ipsilateral middle cerebral artery; *e*, ipsilateral internal carotid bifurcation; *f*, ipsilateral posterior cerebral artery; and *G*, globe.

signals of the ipsilateral A-1 segment, both A-2 segments, and the ipsilateral MCA were red, and the color flow signals of the contralateral MCA were blue. Signals from the contralateral posterior communicating artery and posterior cerebral artery could also be obtained in some subjects. This segment appeared as a blue color.

The frequencies of identifying the OA, each portion of the carotid siphon, contralateral ACA, ipsilateral MCA, and contralateral posterior cerebral artery by transorbital approach are provided in Table 1. Only the contralateral ACA and ipsilateral MCA are shown in Table 1 because they were more easily identified and had an optimal incident angle as compared to the ipsilateral ACA and contralateral MCA. The peak systolic velocities, end-diastolic velocities, and pulsatility indices in various portions of the carotid siphon and major arteries at the base of the brain are provided in Table 2.

Table 3 compares the flow velocities, incident angles, and failure rates between the transtemporal and transorbital approach in detecting the carotid siphon and major arteries at the base of the brain. The incident angles, failure rates, and

end-diastolic flow velocities differed significantly between the two approaches. The failure rate for identifying the ipsilateral anterior cerebral artery was relatively high in the transtemporal approach in contrast to a low failure rate and optimal angle of insonation for the ACA (contralateral) in the transorbital approach. The incident angle for C-3 of the ICA was also smaller in the transorbital approach than in the transtemporal approach. Failure rates varied with the age and sex of the volunteers. Poor transtemporal acoustic window was found in 47.6% (male, 33.3%; female, 66.6%) of the volunteers age 60 or older, as it was in 17.2% (male, 10%; female, 33.3%) of the volunteers younger than age 60 years. Poor transorbital acoustic window was found in 42% (male, 41.6%; female, 44.4%) of the volunteers age 60 years or older, as it was in 24.1% (male, 20.0%; female, 33.3%) of volunteers younger than age 60 years.

Table 4 shows the flow velocities of the MCA, ACA, and various portions of the carotid siphon in 10 volunteers obtained by two examiners. The high correlation demonstrated the repro-

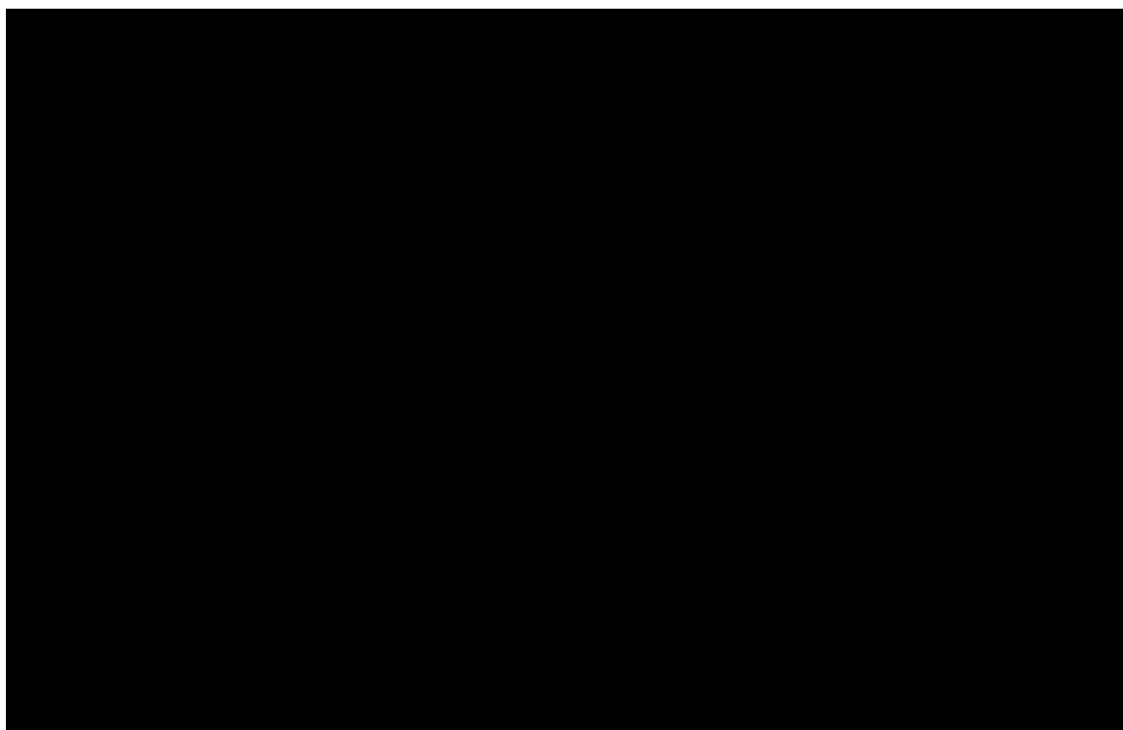


Fig 4. A, Doppler flow imaging of contralateral anterior cerebral artery and middle cerebral artery from the oblique direction of transorbital examination on the left eye.

B, MR angiography of the same subject in corresponding tomographic plane. The letter a indicates right anterior cerebral artery and b, right middle cerebral artery.

ducibility of the transorbital color Doppler flow sonography.

## Discussion

The transorbital Doppler examination (10, 12–14) has been applied in detecting flow sig-

nals from the carotid siphon and other intracranial arteries. However, variations of the distance from the orbital rim to the carotid siphon, MCA, and ACA, and the tortuous and curved course of the arteries, prevent the exact identification of these arterial segment with this “blind method.” In the anteroposterior approach, using this blind method of transorbital Doppler examination (10, 12–16), the flow toward the probe is assumed to come from the carotid siphon at or near the origin of the OA and flow away from the probe, which represents the more distal ICA segment. The oblique approach requires the performance of common carotid compression tests for the verification of vessels (15, 16). Previous experience in the transorbital examination of the ICA and its main branches using a blind technique (10, 12–17) and color Doppler flow imaging provided some knowledge in this study. Various segments of the arteries could be identified using the reference of the anatomic and geographic location in the B scan. On a few occasions, the common carotid artery compression test (11, 16, 17) was needed to make a distinction among the various arteries. The compression tests have been used previously to

TABLE 1: Frequency of identification of the carotid siphon and major arteries at the base of the brain by transorbital approach (N = 50)

Artery	Identification (%)	
	R	L
OA	43 (86)	42 (84)
ICA(C-1)	39 (78)	40 (80)
ICA(C-3)	35 (70)	32 (64)
MCA	36 (72)	38 (76)
ACA(A-1)*	42 (84)	41 (82)
ACA(A-2)	40 (80)	40 (80)
PCA	15 (30)	17 (34)

Note.—OA indicates ophthalmic artery; ICA(C-1), supraclinoid portion of internal carotid artery; ICA(C-3), cavernous sinus portion of internal carotid artery; MCA, middle cerebral artery; ACA(A-1), precommunicating segment of anterior cerebral artery; ACA(A-2), postcommunicating segment of anterior cerebral artery; and PCA, posterior cerebral artery.

\* Contralateral side of ACA(A-1).

**TABLE 2: Normal values for flow velocities and pulsatility indices in the carotid siphon and major arteries at the base of the brain by transorbital approach**

Vessel	n	Depth, mm	Vs, cm/s	Ved, cm/s	RI	A/B Ratio
OA	85	54.9 ± 3.9 (43–61)	48.1 ± 7.2 (39–60)	15.0 ± 5.2 (9–19)	0.66 ± 0.10 (0.22–0.78)	3.01 ± 1.12 (2.21–4.56)
ICA(C-1)	79	67.2 ± 3.9 (63–71)	105.5 ± 25.6 (72–168)	45.5 ± 8.9 (20–60)	0.55 ± 0.06 (0.38–0.68)	2.13 ± 0.36 (1.32–2.97)
ICA(C-3)	67	67.5 ± 6.8 (58–77)	104.1 ± 18.1 (62–146)	45.2 ± 10.7 (23–61)	0.56 ± 0.06 (0.51–0.66)	2.29 ± 0.39 (2.05–2.92)
MCA	74	62.4 ± 9.9 (50–80)	108.2 ± 23.8 (70–166)	44.1 ± 10.1 (26–65)	0.58 ± 0.08 (0.54–0.71)	2.36 ± 0.62 (1.25–3.80)
ACA(A-1)*	83	69.9 ± 4.0 (65–78)	106.5 ± 22.1 (65–168)	43.5 ± 8.4 (22–60)	0.56 ± 0.09 (0.46–0.68)	2.28 ± 0.57 (1.86–3.12)
ACA(A-2)	80	67.6 ± 7.4 (58–80)	88.7 ± 23.1 (60–162)	38.8 ± 9.0 (20–60)	0.57 ± 0.05 (0.52–0.63)	2.57 ± 0.24 (2.33–3.03)
PCA	32	80.3 ± 8.4 (74–90)	72.3 ± 15.8 (30–90)	26.9 ± 6.7 (10–50)	0.63 ± 0.06 (0.49–0.69)	2.48 ± 0.24 (1.96–2.81)

Note.—All parameters are mean ± SD, with range in parentheses; n indicates number of vessels investigated; Depth, distance between the sample volume and transducer; Vs, peak systolic velocity; Ved, end-diastolic velocity; RI, resistance index [(Vs-Ved)/Vs]; and A/B Ratio, Vs/Ved. OA indicates ophthalmic artery; ICA(C-1), supraclinoid portion of internal carotid artery; ICA(C-3), cavernous sinus portion of internal carotid artery; MCA, middle cerebral artery; ACA(A-1), precommunicating segment of anterior cerebral artery; ACA(A-2), postcommunicating segment of anterior cerebral artery; and PCA, posterior cerebral artery.

\* The velocity of ACA(A-1) is measured on the contralateral side.

identify intracranial arteries during the transcranial Doppler examination (12, 16, 17). Signals that came from the MCA were diminished by ipsilateral common carotid artery compression. There should be no change in signal or only a slight augmentation using contralateral common carotid artery compression. Signals from

the A-1 segment of the ACA were diminished or reversed by ipsilateral compression and augmented by contralateral compression. Signals from the ICA were obliterated by ipsilateral common carotid artery compression and augmented by contralateral compression. Signals from the posterior communicating artery were

**TABLE 3: Comparison of flow velocity, incident angle, and failure rate between transorbital and transtemporal approach (N = 100)**

Vessel	Color Doppler Flow Imaging							
	Transtemporal				Transorbital			
	Angle, degree	Vs, cm/s	Ved, cm/s	Failure Rate, %	Angle, degree	Vs, cm/s	Ved, cm/s	Failure Rate, %
ICA(C-1)	49.5 ± 7.8 <sup>†</sup> (36–60)	106.5 ± 12.4 (78–126)	46.1 ± 10.4 (27–66)	23	40.3 ± 4.9 (30–45)	105.5 ± 25.6 (72–168)	45.5 ± 8.9 (20–60)	21
ICA(C-3)*	62.2 ± 7.8 <sup>†</sup> (51–75)	101.2 ± 21.4 (78–129)	40.0 ± 11.7 <sup>†</sup> (31–57)	24 <sup>†</sup>	32.3 ± 4.5 (25–40)	104.1 ± 18.1 (62–146)	45.2 ± 10.7 (23–61)	33
MCA	41.9 ± 8.7 <sup>†</sup> (30–60)	113.2 ± 18.5 (87–152)	51.7 ± 10.8 <sup>†</sup> (30–69)	21 <sup>†</sup>	49.5 ± 10.5 (27–64)	108.2 ± 23.8 (70–166)	44.1 ± 10.1 (26–65)	26
ACA(A-1) <sup>†</sup>	44.1 ± 7.3 <sup>†</sup> (30–59)	106.1 ± 16.1 (80–142)	51.1 ± 12.3 <sup>†</sup> (30–77)	32 <sup>†</sup>	34.0 ± 16.2 (25–60)	106.5 ± 22.1 (60–168)	43.5 ± 8.4 (22–60)	17
ACA(A-2)*	57.0 ± 5.5 <sup>†</sup> (48–69)	85.6 ± 16.2 (58–124)	38.8 ± 10.3 (21–56)	30 <sup>†</sup>	53.0 ± 11.2 (30–64)	88.7 ± 23.1 (60–162)	38.8 ± 9.0 (20–60)	20
PCA	34.5 ± 9.2 (15–55)	76.1 ± 12.1 (58–106)	32.4 ± 9.6 <sup>†</sup> (18–58)	18 <sup>†</sup>	50.1 ± 10.2 (30–64)	72.3 ± 15.8 (30–90)	26.9 ± 6.7 (10–50)	68

Note.—Vs indicates peak systolic velocity with angle correction; Ved, end-diastolic velocity; Angle, velocity with angle correction; Failure Rate, the rate of failure to detect Doppler signals in arteries; ICA(C-1), supraclinoid portion of internal carotid artery; ICA(C-3), cavernous sinus portion of internal carotid artery; MCA, middle cerebral artery; ACA(A-1), precommunicating segment of anterior cerebral artery; ACA(A-2), postcommunicating segment of anterior cerebral artery; and PCA, posterior cerebral artery.

\* Flow velocities were not measured in cases of unknown or unfavorable incident angles.

<sup>†</sup> The velocity and angle of ACA(A-1) in transorbital approach are measured in contralateral side.

<sup>†</sup> Statistically significant difference ( $P < .05$ ) between transtemporal and transorbital approach.

**TABLE 4: Reproducibility of flow velocity measurements in the carotid siphon and major arteries at the base of the brain through transorbital approach**

	n	OA	ICA(C-1)	ICA(C-3)	MCA	ACA(A-1)*	ACA(A-2)
Vs examiner 1	20	42.1 ± 6.1	107.2 ± 10.2	104.5 ± 9.5	110.0 ± 10.1	90.2 ± 16.2	92.2 ± 14.1
examiner 2	20	41.2 ± 5.6	102.1 ± 11.1	100.4 ± 8.0	113.6 ± 15.4	93.3 ± 15.3	90.1 ± 11.4
r		0.78	0.69	0.72	0.74	0.80	0.82
Vd examiner 1	20	15.0 ± 4.1	44.1 ± 7.2	46.5 ± 9.1	60.5 ± 9.2	42.4 ± 12.3	40.5 ± 11.2
examiner 2	20	14.0 ± 3.6	46.2 ± 6.2	43.7 ± 7.3	66.4 ± 9.5	43.6 ± 9.1	42.1 ± 10.7
r		0.82	0.72	0.74	0.76	0.82	0.78

Note.—Values of both measurements are mean ± SD. n indicates number of vessels investigated; OA, ophthalmic artery; ICA(C-1), supraclinoid portion of internal carotid artery; ICA(C-3), cavernous sinus portion of internal carotid artery; MCA, middle cerebral artery; ACA(A-1), contralateral side precommunicating segment of anterior cerebral artery; Vs, peak systolic velocity; Vd, end-diastolic velocity; and r, intraclass correlation coefficient.

\* The velocities of ACA(A-1) are measured in contralateral side.

not obliterated by common carotid artery compression. In this study, we successfully obtained high detection rates and clear images of the carotid siphon and the major arteries at the base of the brain by transorbital color Doppler flow sonography.

The transtemporal approach of transcranial Doppler examination has been reported to fail in 2% to 30% of the subjects (7–10). It is attributed to the poor acoustic window; failure occurs more frequently in female, black, and Asian subjects (7, 9, 10). In this work, transorbital color Doppler flow sonography was demonstrated to have lower failure rates than the transtemporal approach in identifying the ACA and the carotid siphon (Table 3). Using the transorbital approach, a better color imaging was obtained as compared with the transtemporal approach. Five volunteers, who had no temporal acoustic windows and had completely unsuccessful examinations using the transtemporal approach, had successful color imaging and detection of flow velocities in the ICA, MCA, and ACA using the transorbital approach.

Even in patients with a good temporal acoustic window, the transorbital color Doppler flow examination is still important in evaluating the carotid siphon and the ACA at an optimum Doppler incident angle. The Doppler incident angles with transtemporal approach for the ICA (C-3 and A-1) were often quite unfavorable (ie, more than 64°) (Table 3). These angles do not allow an accurate measurement of Doppler flow velocities. Moreover, Tsuchiya et al (2) reported that with the transtemporal approach using color Doppler flow imaging, the MCA was readily identified in all their 50 subjects, whereas the ACA was identified in only 7 of the 50. In our study, the transorbital approach

had higher identification rates and smaller incident angles for ICA (C-3) and ACA. Therefore, the transorbital approach can add flow data to those already obtained from the transtemporal examination.

The blood-flow direction and velocity of the OA determined by current Doppler examination has been used for the diagnosis of occlusive carotid disease and evaluation of the collateral circulation (18–25). Reversed blood-flow direction in the ipsilateral OA is frequently detected in patients with occlusion or tight stenosis of the ICA. However, forward flow in the OA was occasionally found in patients with similar carotid disease. This forward Doppler OA flow has been explained by intracranial collaterals from the contralateral carotid or vertebrobasilar system. Another explanation for this forward OA flow is the collateral flow from the middle meningeal artery (26–28). Under such situations, the flow reversal could occur only in the proximal segment or near the origin of the OA (27, 28). The reversal of the OA flow would be missed in the Doppler examination, which insonates only the middle portion of the OA. The proximal segment of the OA and the junction of the carotid siphon and OA are therefore important areas for Doppler insonation, which can be accomplished via the transorbital color Doppler flow examination (there was 85% identification rate of the origin of the OA in this work).

Safety and the potential hazard associated with this transorbital ultrasound examination are of primary concern. In this study, we instructed the subjects to turn their eyes away from the probe during the test and the probe was applied on the lateral or superior orbital rim. This design not only avoids the refractive power of the lens, but also prevents ultrasound

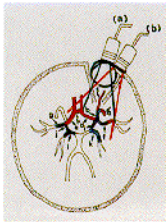


beams' being directed at the lens of the subject. For safety, the low power setting ( $<25$  or  $<50$  mW/cm<sup>2</sup>) was used, and the maximal insonation time for each eye was 20 minutes. Continuous-wave ultrasound with a 50 mW/cm<sup>2</sup> power setting for studying the OA has been used in our laboratory for 12 years on at least 25 000 patients without complaints or known adverse effects. The safety of transorbital ultrasound examination has been discussed previously in literature and is believed to be safe for the eyes (12, 14, 18, 29, 30).

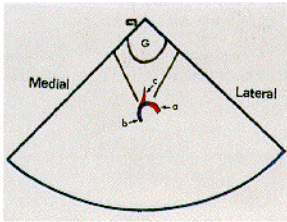
In conclusion, we have found that the transorbital color Doppler flow imaging is particularly useful for the study of flow and imaging of the ACA (contralateral) and anterior communicating artery as well as for the study of collateral circulation through the OA and anterior communicating artery. This approach can add to the information provided from a transtemporal examination and is also an alternative way to study the MCA in patients with a poor acoustic window in the temporal bone.

## References

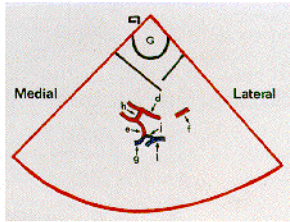
1. Bogdahn U, Becker G, Winkler J, Greiner K, Perez J, Meurers B. Transcranial color-coded real-time sonography in adults. *Stroke* 1990;21:1680-1688
2. Tsuchiya T, Yasaka M, Yamaguchi T, Kimura K, Omae T. Imaging of the basal cerebral arteries and measurement of blood velocity in adults by using transcranial real-time color flow Doppler sonography. *AJNR Am J Neuroradiol* 1991;12:497-502
3. Kaps M, Seidel G, Bauer T, Behrmann B. Imaging of the intracranial vertebrobasilar system using color-coded ultrasound. *Stroke* 1992;23:1577-1582
4. Schoning M, Walter J. Evaluation of the vertebrobasilar-posterior system by transcranial color duplex sonography in adults. *Stroke* 1992;23:1280-1286
5. Becker G, Greiner K, Kaune B, et al. Diagnosis and monitoring of subarachnoid hemorrhage by transcranial color-coded real-time sonography. *Neurosurgery* 1991;28:814-820
6. Becker G, Winkler J, Hoffmann E, Bogdahn U. Imaging of cerebral arterio-venous malformations by transcranial colour-coded real-time sonography. *Neuroradiology* 1990;32:280-288
7. Eden A. Transcranial Doppler ultrasonography and hyperostosis of the skull. *Stroke* 1988;19:1445-1446
8. Halsey JH. Effect of emitted power on waveform intensity in transcranial Doppler. *Stroke* 1990;21:1573-1578
9. Eden A. Effect of emitted power on waveform intensity in transcranial Doppler. *Stroke* 1991;22:533
10. Wong WJ, Hu HH, Lo YK, Luk YO, Chen CM. Transcranial Doppler in cerebrovascular disease. In: Oka M, von Reutern G.-M., Furuhashi H, Kodaira K, eds. *Recent Advances in Neurosonology*. New York: International Congress Series, 1992:113-118
11. Spencer MP, Whisler D. Transorbital Doppler diagnosis of intracranial arterial stenosis. *Stroke* 1986;17:916-921
12. Lindegaard KF, Bakke SJ, Aaslid R, Nornes H. Doppler diagnosis of intracranial artery occlusive disorders. *J Neurol Neurosurg Psychiatry* 1986;49:510-518
13. Ley-Pozo J, Ringelstein EB. Noninvasive detection of occlusive disease of the carotid siphon and middle cerebral artery. *Ann Neurol* 1990;28:640-646
14. Aaslid R. Transcranial Doppler examination techniques. In: Aaslid R, ed. *Transcranial Doppler Sonography*. Vienna & New York: Springer-Verlag, 1986:39-59
15. Fujioka KA, Douville CM. Anatomy and freehand examination techniques. In: Newell DW, Aaslid R, eds. *Transcranial Doppler*. New York: Raven, 1992:26-27
16. Ringelstein EB, Kahlscheuer B, Niggemeyer E, Otis SM. Transcranial Doppler sonography: anatomical landmarks and normal velocity values. *Ultrasound Med Biol* 1990;16:745-761
17. Lindegaard KF. Indices of pulsatility. In: Newell DW, Aaslid R, eds. *Transcranial Doppler*. New York: Raven, 1992:67-82
18. Hu HH, Sheng WY, Yen MY, Lai ST, Teng MM. Color Doppler imaging of orbital arteries for detection of carotid occlusive disease. *Stroke* 1993;24:1196-1203
19. Tatemichi TK, Chamorro A, Petty GW, et al. Hemodynamic role of ophthalmic artery collateral in internal carotid artery occlusion. *Neurology* 1990;40:461-464
20. Strauss AL, Rieger H, Roth FJ, Schoop W. Doppler ophthalmic blood pressure measurement in the hemodynamic evaluation of occlusive carotid artery disease. *Stroke* 1989;20:1012-1015
21. Hodek-Demarin V, Muller HR. Reversed ophthalmic artery flow in internal carotid artery occlusion: a re-appraisal based on ultrasonic Doppler investigations. *Stroke* 1979;10:461-463
22. Kaneda H, Irino T, Arita N, Minami T, Taneda M, Shiraishi J. Relationship between ophthalmic artery blood flow and recanalization of occluded carotid artery: ultrasonic Doppler study. *Stroke* 1978;9:360-363
23. Maroon JC, Campbell RL, Dyken ML. Internal carotid artery occlusion diagnosed by Doppler ultrasound. *Stroke* 1970;1:122-127
24. Brucher J. Origin of the ophthalmic artery from the middle meningeal artery. *Radiology* 1969;93:51-52
25. Sawamura Y, Nakagawa Y, Sakuragi M, Shima K, Sugimoto S, Tsuru M. Internal carotid artery occlusion diagnosed by Doppler ultrasound. *Neurol Surg* 1984;12:377-381
26. Dilenge D, Archerl GF Jr. Variations of the ophthalmic and middle meningeal arteries: relation to the embryonic stapodial artery. *AJNR Am J Neuroradiol* 1980;1:45-53
27. Lee TH, Ryn SH, Chen ST, Liu YH, Tzeng KY. Forward Doppler ophthalmic flow in patients with internal carotid artery occlusion. In: Oka M, von Reutern G.-M., Furuhashi H, Kodaira K, eds. *Recent Advances in Neurosonology*. New York: International Congress Series, 1992:401-404
28. Muller HR. Directional Doppler sonography: a new technique to demonstrate flow reversal in the ophthalmic artery. *Neuroradiology* 1973;5:91-94
29. Lizzi FL, Mortimer AJ. Bioeffects considerations for the safety of diagnostic ultrasound. *J Ultrasound Med* 1988;7(suppl):1-38
30. Lie WE, Cohen SM, Merton DA, Shields JA, Mitchell DG, Goldberg BB. Color Doppler imaging of the eye and orbit: technique and normal vascular anatomy. *Arch Ophthalmol* 1991;109:527-531



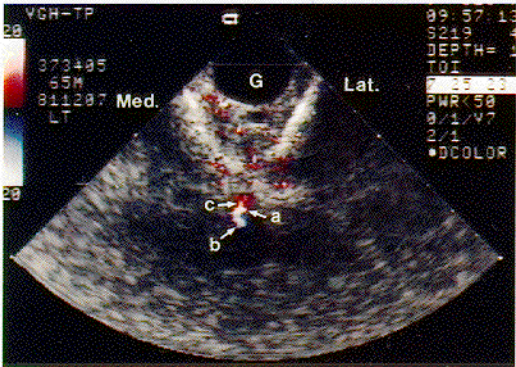
A



B



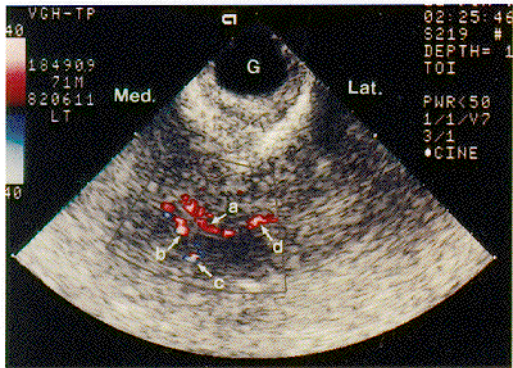
C



A



B



Med.

Lat.

G

23

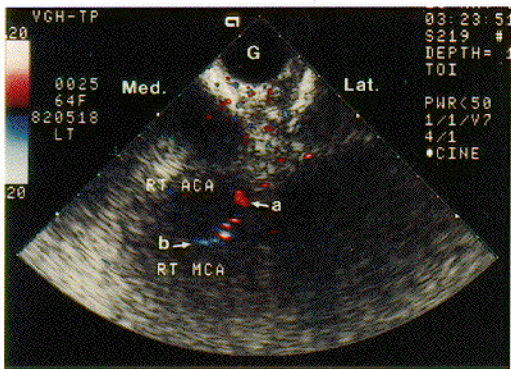
24

25

26

B





A

